

TRAVELING WAVES AND THEIR EVOLUTION FOR THE ZK(N,2N,-N) EQUATION*

Feiting Fan¹, Yuqian Zhou² and Xingwu Chen^{1,†}

Abstract In this paper, using the approach of dynamical systems we investigate the traveling waves for the ZK(n,2n,-n) equation including the types and evolution of traveling waves. The traveling wave problem is converted into the analysis of phase portraits of the corresponding traveling wave system, which is 5-parametric and has a singular line in its phase space. The orbits passing through this singular line in phase portraits are determined by a time rescaling. After converting the orbits in these phase portraits into traveling waves, we state all types of traveling waves and give at least one exact traveling wave solution for each type of bounded traveling waves in our main results. Finally, we discuss the evolution of these traveling waves among themselves when parameters vary by the bifurcations happening in the phase portraits of the traveling wave system.

Keywords Compacton, solitary wave, solitary cusp wave, traveling wave, ZK(n,2n,-n) equation.

MSC(2010) 34C37, 34C23, 58Z05, 74J30.

1. Introduction and main results

Concerning solutions of partial differential equations, one of important topics is traveling wave solution (see, e.g., [4, 5, 10, 14, 28, 29]), a kind of solutions moving with constant speeds in some direction.

The well-known integrable nonlinear Korteweg-de Vries (KdV) equation (see [8])

$$u_t + uu_x + u_{xxx} = 0 \quad (1.1)$$

is an important model to describe the evolution of the weakly nonlinear steepening and the weakly dispersive wave that appears in many applications, such as surface waves in shallow water, acoustic waves, heat pulses in anharmonic crystals, ion-acoustic wave, and magneto-sonic waves in a magnetized plasma (see, e.g., [7, 16, 20]). In equation (1.1), the nonlinear convection term uu_x causes the steepening of wave form and the linear dispersion effect term u_{xxx} makes the wave form spread. Moreover, the balance between this weak nonlinear steepening and the linear dispersion

[†]The corresponding author. Email: xingwu.chen@hotmail.com(X. Chen)

¹Department of Mathematics, Sichuan University, Chengdu 610064, China

²College of Applied Mathematics, Chengdu University of Information Technology, Chengdu 610225, China

*The second author was supported by the China Postdoctoral Science Foundation (No. 2016M602663) and the third author was supported by National Natural Science Foundation of China (No. 11871355).

gives rise to solitons: localized waves without change of its shape and velocity properties during propagation and after mutual collisions (see [31]).

In 1993, seeking to understand the role of nonlinear dispersion in the formation of nonlinear structures like liquid drops, Rosenau and Hyman in [19] introduce and study a family of fully nonlinear KdV equations, denoted by $K(n,n)$:

$$u_t + a(u^n)_x + (u^n)_{xxx} = 0, \quad n > 1.$$

They found that for certain n , the delicate interaction between nonlinear convection $(u^n)_x$ with the genuine nonlinear dispersion $(u^n)_{xxx}$ generates solitary waves with exact compact support. That is, these particle-like waves vanish identically outside a finite core region. Just as the suffix-on is used in modern physics to indicate the particle property (such as phonon, photon, soliton, etc.), they call this type of solitary wave *compacton*: solitons with finite wavelengths or solitons free of exponential tails (see, e.g., [19, 21, 22]). Different from the soliton collisions in an integrable system, compactons reemerge with the same coherent shape after colliding with other compactons. Later in [18] in 1994, Rosenau pointed out that compactons arise in a wide variety of settings where nonlinear dispersion arises naturally, but the underlying nonlinear mechanism responsible for the coherence and robustness of interaction remains very much a mystery. Moreover, unlike the bell-shaped solitary wave, compacton as a type of “new wave” is a nonanalytic wave. These complex but interesting discoveries have attracted many scholars to study the compacton (see, e.g., [21, 22]).

An extensive research work has been done in developing higher dimensional models, particularly those in the (2+1) dimension, i.e., two spatial and one time. As a well-known generalization of (1.1), the nonintegrable Zakharov-Kuznetsov (ZK) equation

$$u_t + auu_x + b(u_{xx} + u_{yy})_x = 0, \quad (1.2)$$

was first derived in [32] in 1974 and was used to describe weakly nonlinear ion-acoustic waves in a strongly magnetized lossless plasma comprising cold ions and hot isothermal electrons in [15, 17]. Various useful techniques have been devoted to traveling waves of (1.2), such as the extended tanh method in [12, 26], sine-cosine method in [23], sine-cosine ansatz in [24], solitary wave ansatz method in [2] and extended hyperbolic function method in [3].

Motivated by the rich treasure of the ZK equation in the literature and the interest in compacton, we will study a nonlinear dispersive equation, a special type of the ZK equation, of the form

$$u_t + a_0(u^n)_x + [b_0u^{-n}(u^{2n})_{xx} + c_0(u^n)_{yy}]_x = 0 \quad (1.3)$$

and

$$u_t + a_0(u^n)_x + [b_0u^{2n}(u^{-n})_{xx} + c_0(u^n)_{yy}]_x = 0, \quad (1.4)$$

where a_0, b_0, c_0 are three non-zero real numbers and play a major role in change of the physical structures of their solutions, n is an integer greater than 1 (see [25]). Equations (1.3), (1.4) are usually called as $ZK(n,-n,2n)$, $ZK(n,2n,-n)$, respectively. As in [1], the first term is the evolution term, the second term is the nonlinear term while the third and fourth terms together form the nonlinear dispersion terms. Compactons solutions and solitary patterns solutions of equations (1.3) and (1.4) were obtained in [25] by the sine-cosine method and the tanh method. One can

find results about semi-traveling wave solutions in [9], bright soliton solutions and the Jacobi elliptic function solutions in [1, 30], and group-invariant solutions in [6]. For $n = 2$, some results about periodic traveling wave solutions are given in [27] for equation (1.4). However, we note that the traveling waves of equations (1.3) and (1.4) with general n have not been discussed completely in the relevant literatures, especially for their non-smooth traveling waves. Moreover, there is no results about the evolvement among different traveling waves when parameters vary, which is helpful for us to understand these traveling waves.

It is the objective of this work to investigate the traveling waves of equation (1.4) including their types and evolution by the approach of dynamical systems. Substituting $u(x, y, t) = \phi(x + ay - ct) = \phi(\xi)$ into (1.4) and integrating it, we get

$$-c\phi + a_0\phi^n + A\phi^{n-2}(\phi')^2 + B\phi^{n-1}\phi'' = g, \tag{1.5}$$

where $'$ denotes the derivative with respect to ξ , g is an integral constant, $A := b_0n(n + 1) + a^2c_0n(n - 1)$, $B := a^2c_0n - b_0n$ and $ac \neq 0$. When $B = 0$, equation (1.5) is a one-dimensional differential equation of order 1. When $B \neq 0$, equation (1.5) is equivalent to the following planar Hamiltonian system

$$\frac{d\phi}{d\xi} = y, \quad \frac{dy}{d\xi} = \frac{-A\phi^{n-2}y^2 - a_0\phi^n + c\phi + g}{B\phi^{n-1}}. \tag{1.6}$$

Since (1.6) is invariant under $(A, B, a_0, c, g) \rightarrow (-A, -B, -a_0, -c, -g)$, we need only to consider $c > 0$. Moreover, (1.6) is invariant under $(\xi, \phi, A, B, a_0, c, g) \rightarrow (-\xi, -\phi, -A, -B, -a_0, c, -g)$ when n is even. Thus, we assume in system (1.6) that $(A, B, a_0, c, g) \in \Omega := \{(A, B, a_0, c, g) \in \mathbb{R}^5 : a_0B \neq 0, c > 0\}$ when n is odd and $(A, B, a_0, c, g) \in \tilde{\Omega} := \{(A, B, a_0, c, g) \in \mathbb{R}^5 : B \neq 0, a_0 > 0, c > 0\}$ when n is even. Clearly, y -axis in the phase space (ϕ, y) is a singular line except the special case that $n - 2 = g = A = 0$, which corresponds to system

$$\frac{d\phi}{d\xi} = y, \quad \frac{dy}{d\xi} = \frac{-a_0\phi + c}{B}. \tag{1.7}$$

System (1.7) is linear and easy to get its solutions. In the case that $g = 0$, system (1.6) can be written as

$$\frac{d\phi}{d\xi} = y, \quad \frac{dy}{d\xi} = \frac{-Ay^2 - a_0\phi^2 + c\phi}{B\phi}, \quad A \neq 0, \tag{1.8}$$

$$\frac{d\phi}{d\xi} = y, \quad \frac{dy}{d\xi} = \frac{-Ay^2 - a_0\phi^2 + c}{B\phi}, \tag{1.9}$$

$$\frac{d\phi}{d\xi} = y, \quad \frac{dy}{d\xi} = \frac{-A\phi^{n-3}y^2 - a_0\phi^{n-1} + c}{B\phi^{n-2}} \tag{1.10}$$

when $n = 2, 3, \geq 4$, respectively. In the case that $g \neq 0$, system (1.6) can be written as

$$\frac{d\phi}{d\xi} = y, \quad \frac{dy}{d\xi} = \frac{-Ay^2 - a_0\phi^2 + c\phi + g}{B\phi}, \tag{1.11}$$

$$\frac{d\phi}{d\xi} = y, \quad \frac{dy}{d\xi} = \frac{-A\phi^{n-2}y^2 - a_0\phi^n + c\phi + g}{B\phi^{n-1}} \tag{1.12}$$

when $n = 2, \geq 3$, respectively.

We give completed orbit structures in phase space (ϕ, y) for systems (1.8)-(1.12) in Section 2 by the planar dynamical method. From these phase portraits, we get the information of traveling wave solution $u(x, y, t) = \phi(x + ay - ct)$ of equation (1.4) including wave graphs and some exact expressions.

Theorem 1.1. *For traveling wave solution $u(x, y, t) = \phi(x + ay - ct)$ of equation (1.4) satisfying $a^2 \neq b_0/c_0$ and $ac \neq 0$, all wave graphs are given in Figure 1 for the bounded case and in Figure 2 for the unbounded case.*

In Figure 1 we observe that there are 7 classes of bounded traveling waves (see, e.g., [11, 13]), i.e., *compacton* (Figure 1(1-1)), *periodic wave* (Figures 1(1-2)-(1-4)), *periodic cusp wave* (Figures 1(1-5)-(1-6)), *solitary wave* (Figures 1(1-7)-(1-10)), *solitary cusp wave* (Figures 1(1-11)-(1-12)), *two-sided breaking wave* (Figures 1(1-13)-(1-14)) and *one-sided breaking kink/anti-kink wave* (Figures 1(1-15)-(1-18)). For these 7 classes of bounded traveling waves, we give their exact expressions.

Theorem 1.2. *Equation (1.4) satisfying $a^2 \neq b_0/c_0$ and $ac \neq 0$ has bounded traveling wave solutions*

$$\phi(\xi) = \frac{3c}{2a_0} \cos^2 \left(\sqrt{\frac{a_0}{6B}} \xi \right) \quad (1.13)$$

of type compacton,

$$\phi(\xi) = \frac{r_1 r_2}{r_2 - (r_2 - r_1) \operatorname{sn}^2 \left(\sqrt{\frac{-h_1 r_2}{2B}} \xi, \hat{k} \right)} \quad (1.14)$$

of type periodic wave,

$$\phi(\xi) = \frac{3c + \sqrt{9c^2 + 48a_0 g}}{4a_0} - \frac{\sqrt{9c^2 + 48a_0 g} \left(\exp \left(\sqrt{\frac{2a_0}{-3B}} \xi \right) + 1 \right)^2}{8a_0 \exp \left(\sqrt{\frac{2a_0}{-3B}} \xi \right)} \quad (1.15)$$

of type periodic cusp wave,

$$\phi(\xi) = r_4 - \frac{4(r_4 - r_3) \exp \left(\sqrt{\frac{2h_2(r_4 - r_3)}{B}} \xi \right)}{\left(1 + \exp \left(\sqrt{\frac{2h_2(r_4 - r_3)}{B}} \xi \right) \right)^2} \quad (1.16)$$

of type solitary wave,

$$\phi(\xi) = \frac{3c}{4a_0} \left(1 - \exp \left(-\sqrt{\frac{2a_0}{-3B}} |\xi| \right) \right) \quad (1.17)$$

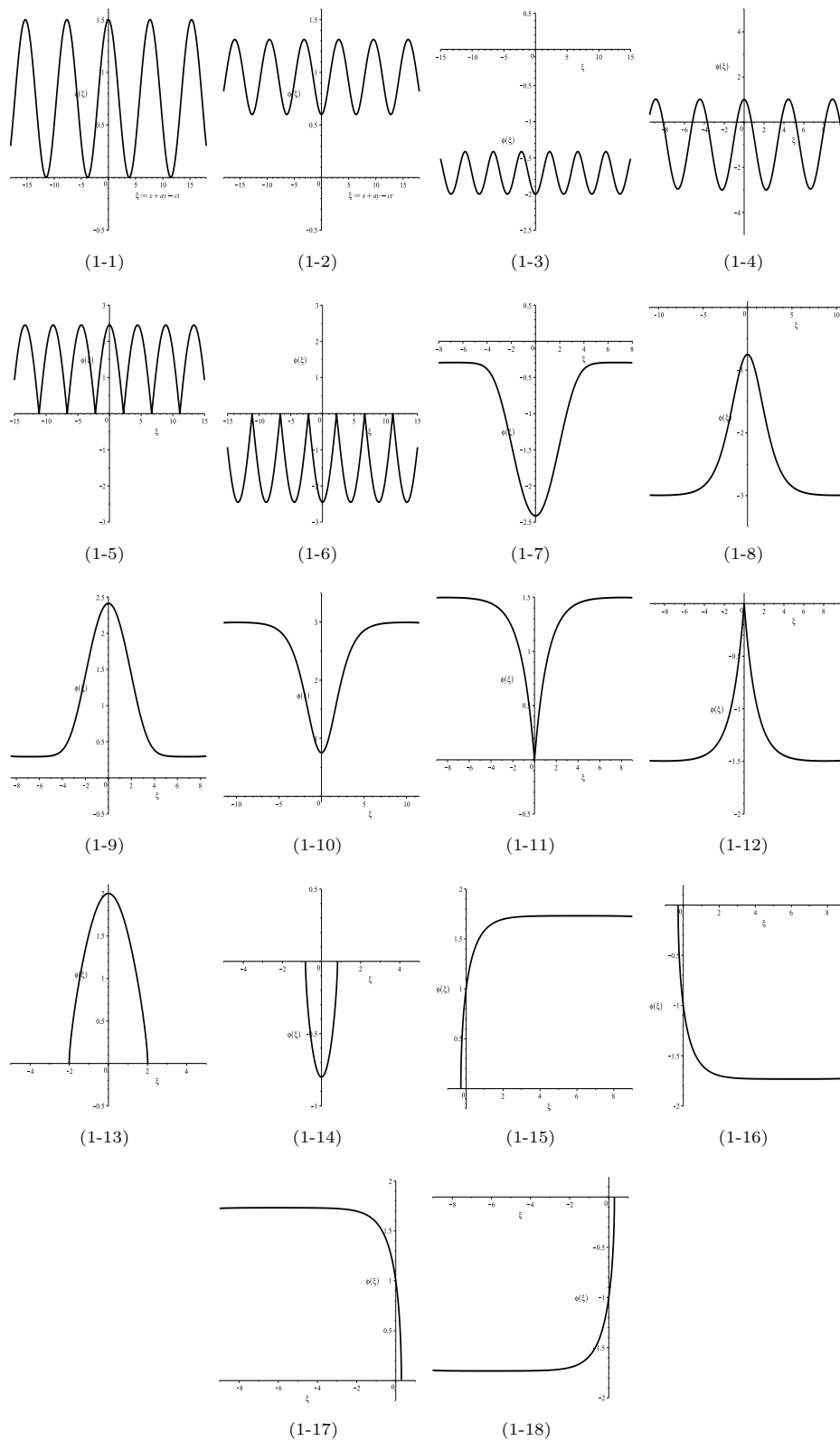


Figure 1. Graphs of bounded traveling waves for equation (1.4).

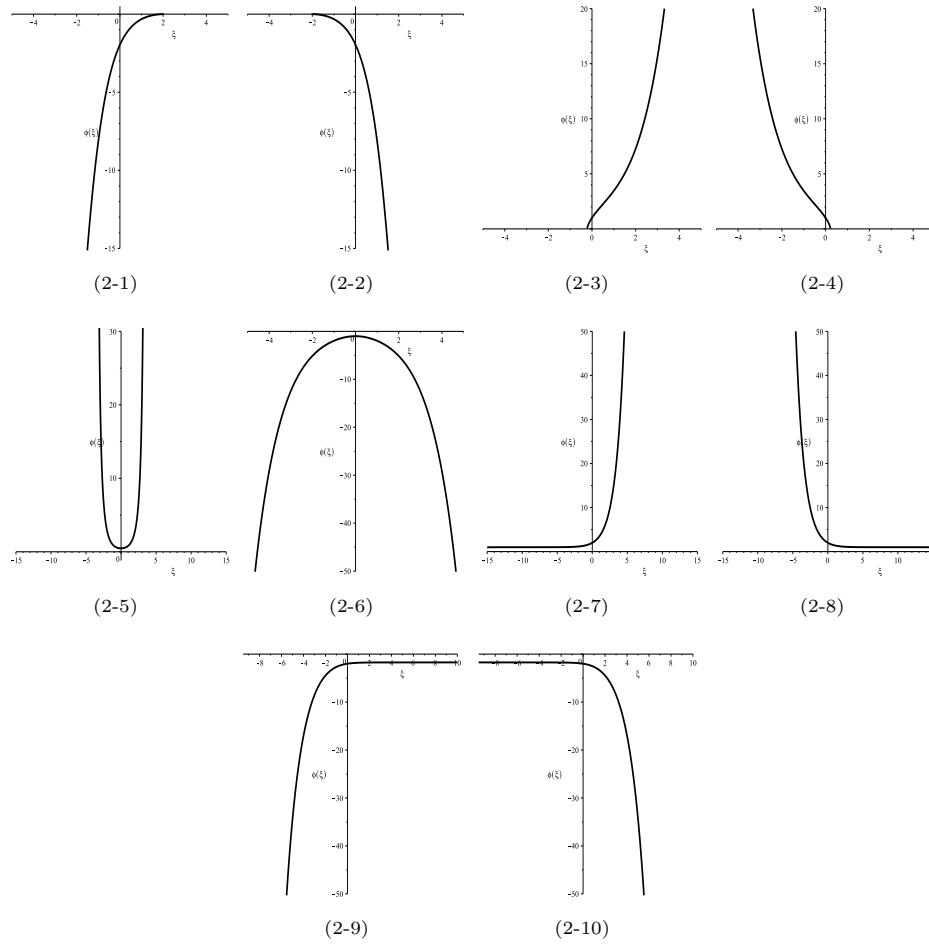


Figure 2. Graphs of unbounded traveling waves for equation (1.4).

of type solitary cusp wave,

$$\begin{aligned} \phi(\chi) &= -\frac{r_5 A_1 (1 + \operatorname{cn}(\chi, k))}{(B_1 - A_1)(1 + \operatorname{cn}(\chi, k)) - 2B_1}, \\ \xi(\chi) &= \sqrt{\frac{3B}{2a_0 A_1 B_1}} \left(\frac{r_5 A_1}{B_1 - A_1} \chi - \frac{r_5 (A_1 + B_1)}{2(B_1 - A_1)} \Pi \left(\arccos(\operatorname{cn}(\chi, k)), \frac{\alpha^2}{\alpha^2 - 1}, k \right) \right) \\ &\quad - \sqrt{\frac{3B}{2a_0}} \arctan \left(\frac{r_5}{2\sqrt{A_1 B_1}} \operatorname{sd}(\chi, k) \right) \end{aligned} \tag{1.18}$$

of type two-sided breaking wave,

$$\begin{aligned} \phi(\chi) &= \frac{c}{2a_0} \cdot \frac{\chi^2}{\chi^2 + 1}, \\ \xi(\chi) &= \sqrt{\frac{6B}{a_0}} (\chi - \arctan(\chi)) \end{aligned} \tag{1.19}$$

of type one-sided breaking kink wave, where $\xi = x + ay - ct$, all $\text{sn}(\cdot, \hat{k})$, $\text{cn}(\cdot, k)$, $\text{sd}(\cdot, k)$ are elliptic integrals of the first kind, $\Pi(\cdot, \alpha^2/(\alpha^2 - 1), k)$ is the elliptic integral of the third kind and $0 < r_1 < c/a_0 < r_2, 0 < r_3 < (c - \sqrt{c^2 + 4a_0g})/(2a_0) < r_4 = (c + \sqrt{c^2 + 4a_0g})/(2a_0), 0 < r_5 < c/(2a_0), -a_0^2/(2c) < h_1 < 0, h_2 = -(3a_0^2c^2 + 8a_0^3g + 3a_0^2c\sqrt{c^2 + 4a_0g})/(6c^3 + 18a_0cg + 6(c^2 + 4a_0g)^{3/2}), A_1, B_1, \alpha, \hat{k}, k$ satisfy $A_1^2 = 3r_5^2 - 3cr_5/a_0 + 3c^2/(4a_0^2), B_1^2 = r_5^2 - 3cr_5/(2a_0) + 3c^2/(4a_0^2), \alpha = (A_1 - B_1)/(A_1 + B_1), \hat{k}^2 = (r_2 - r_1)/r_2, k^2 = (r_5^2 - (A_1 - B_1)^2)/(4A_1B_1)$.

This paper is organized as follows. In Section 2, we analyze the orbit structures in phase space (ϕ, y) for systems (1.8)-(1.12) and then give a proof of Theorem 1.1. In Section 3, for these 7 classes of bounded traveling waves shown in Figure 1 we obtain their exact expressions and hence finish the proof of Theorem 1.2. Finally, in Section 4 conclusions are summarized and a remark is given for the evolution of these traveling waves. Moreover, some simulations are done to illustrate our theoretical results.

2. Phase portrait analysis and proof of Theorem 1.1

In order to get the information of traveling wave solution $u(x, y, t) = \phi(x + ay - ct)$ of equation (1.4), in this section we analyze the orbit structures in phase space (ϕ, y) for systems (1.8)-(1.12) and then finish the proof of Theorem 1.1.

Lemma 2.1. (1) System (1.8) has a unique equilibrium, which lies at $P_1(c/a_0, 0)$ and is a center (resp. saddle) if $B > 0$ (resp. $B < 0$). The phase portraits are given in Figure 3;

(2) System (1.9) has no equilibrium when $a_0 < 0$ and exactly two equilibria when $a_0 > 0$. These two equilibria lie at $P_{2,3}(\pm\sqrt{c/a_0}, 0)$ and are two centers (resp. two saddles) if $B > 0$ (resp. $B < 0$). The phase portraits are given in Figure 4;

(3) System $(1.10)_{n=2m}$ has a unique equilibrium, which lies at $P_4((c/a_0)^{1/(2m-1)}, 0)$ and is a center (resp. saddle) if $B > 0$ (resp. $B < 0$). System $(1.10)_{n=2m+1}$ has no equilibrium when $a_0 < 0$ and exactly two equilibria when $a_0 > 0$. These two equilibria lie at $P_{5,6}(\pm(c/a_0)^{1/(2m)}, 0)$ and are two centers (resp. saddles) if $B > 0$ (resp. $B < 0$). Here $m \geq 2$. The phase portraits of systems $(1.10)_{n=2m}$ and $(1.10)_{n=2m+1}$ are given in Figures 5 and 6, respectively.

Proof. In order to analyze systems (1.8), (1.9) and (1.10), which have a singular line $\phi = 0$, we change (1.8) and (1.9) into

$$\frac{d\phi}{d\zeta} = B\phi y, \quad \frac{dy}{d\zeta} = -Ay^2 - a_0\phi^2 + c\phi, \quad A \neq 0, \tag{2.1}$$

$$\frac{d\phi}{d\zeta} = B\phi y, \quad \frac{dy}{d\zeta} = -Ay^2 - a_0\phi^2 + c \tag{2.2}$$

by $d\xi = B\phi d\zeta$ and change (1.10) into

$$\frac{d\phi}{d\zeta} = B\phi^{n-2}y, \quad \frac{dy}{d\zeta} = -A\phi^{n-3}y^2 - a_0\phi^{n-1} + c \tag{2.3}$$

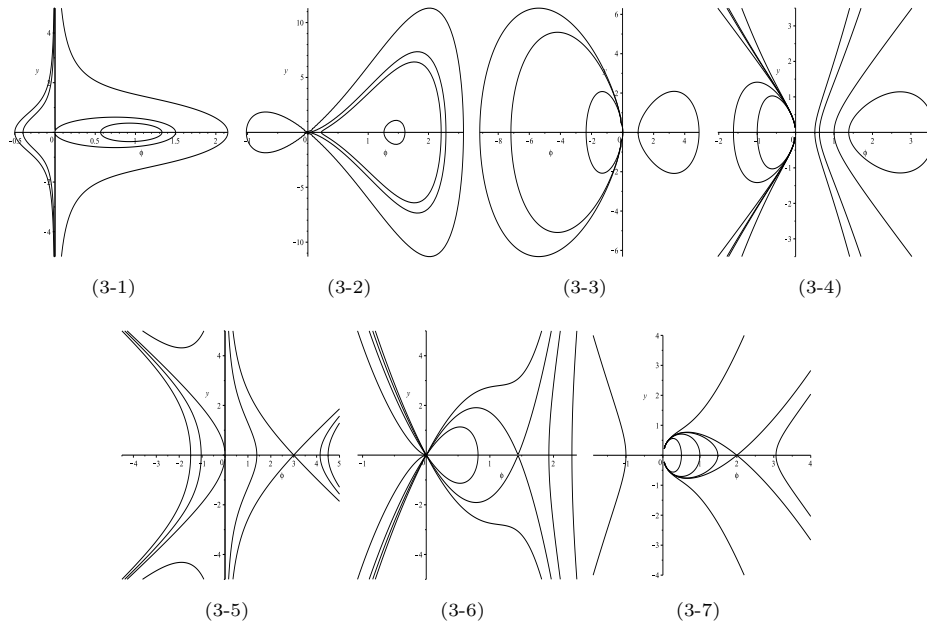


Figure 3. Phase portraits of system (1.8).

by $d\xi = B\phi^{n-2}d\zeta$. Clearly, systems (1.8), (1.9) and (1.10) are equivalent to systems (2.1), (2.2) and (2.3), respectively, except on the y -axis. Straight computation shows that system (2.1) has exactly two equilibria, which lie at $O(0, 0)$ and $P_1(c/a_0, 0)$. Moreover, O corresponds to a degenerate coefficient matrix and P_1 has characteristic equation $\lambda^2 + Bc^2/a_0 = 0$. Thus, O is a degenerate equilibrium and P_1 is a center (resp. saddle) if $B > 0$ (resp. $B < 0$) for system (2.1), which means that the statement about equilibria for system (1.8) is proven. In order to get the orbit structures in (ϕ, y) , by $v = y, w = \phi - Ay^2/c - a_0\phi^2/B, t = c\zeta$, we change (2.1) into

$$\frac{dv}{dt} = w, \quad \frac{dw}{dt} = \frac{AB}{c^2}v^3 \left(1 + \frac{a_0A}{c^2}v^2 + \dots \right) - \frac{2A}{c}vw. \quad (2.4)$$

By [33, P. 132, Theorem 7.2], O of system (2.4) is a saddle if $AB < 0$. Moreover, a small neighborhood of O consists of an elliptical sector and a hyperbolic sector if $AB > 0$, so does (2.1). Conclusion (1) is proven.

For system (2.2), we have four equilibria when $a_0 > 0$ and $A > 0$, which lie at $P_{2,3}(\pm\sqrt{c/a_0}, 0)$ and $Q_{\pm}(0, \pm\sqrt{c/A})$. Then, P_2 and P_3 have the same characteristic equation $\lambda^2 + 2Bc = 0$ and Q_{\pm} have characteristic equations $\lambda^2 \pm (2\sqrt{Ac} - B\sqrt{c/A})\lambda - 2Bc = 0$ respectively. By the theory of planar dynamical systems, $P_{2,3}$ are two centers and Q_{\pm} are two saddles when $B > 0$; $P_{2,3}$ are two saddles and Q_{\pm} are two nodes when $B < 0$. Conclusion (2) is proven.

It is not hard to find that system $(2.3)_{n=2m}$ has a unique equilibrium, lying at $P_4((c/a_0)^{1/(2m-1)}, 0)$, and system $(2.3)_{n=2m+1}$ has no equilibrium when $a_0 < 0$ and exactly two equilibria when $a_0 > 0$, which lie at $P_{5,6}(\pm(c/a_0)^{1/(2m)}, 0)$. By the characteristic equations of P_4, P_5, P_6 , we get that $P_{4,5,6}$ are centers (resp. saddles) if $B > 0$ (resp. $B < 0$). Conclusion (3) is proven. Finally, by the information of

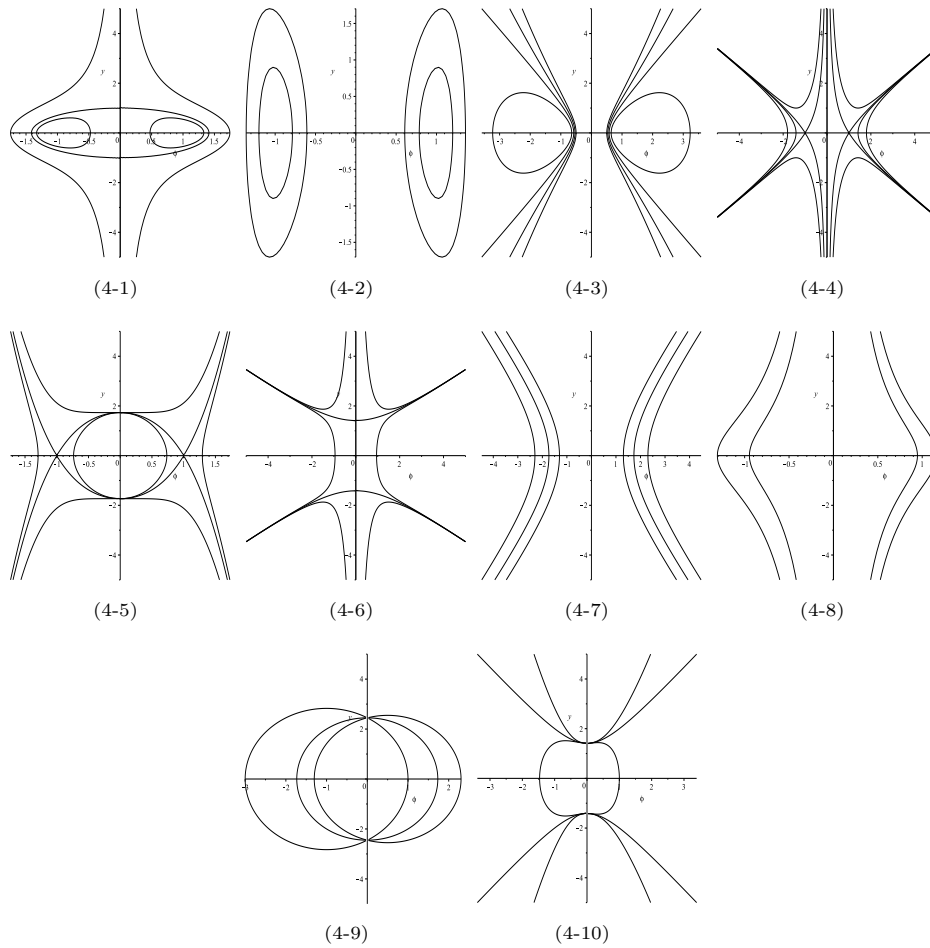


Figure 4. Phase portraits of system (1.9).

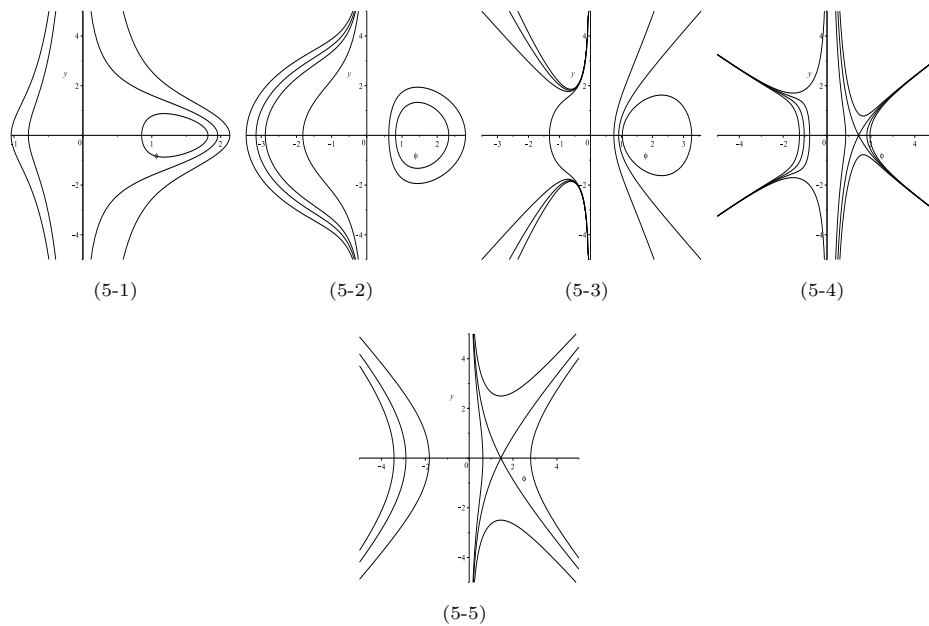


Figure 5. Phase portraits of (1.10) for even $n \geq 4$.

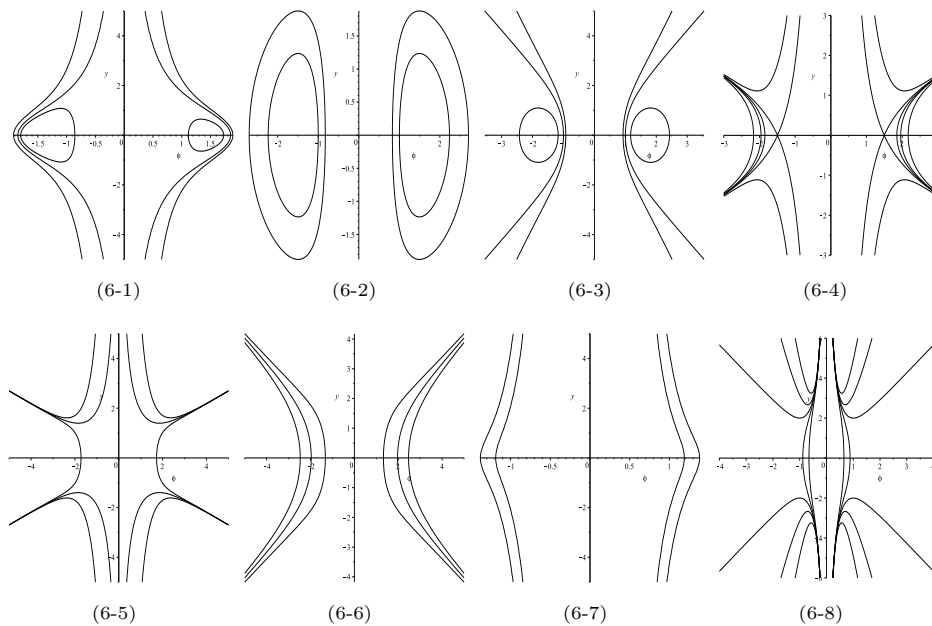


Figure 6. Phase portraits of (1.10) for odd $n \geq 5$.

(2.1), (2.2) and (2.3) we get phase portraits of (1.8), (1.9) and (1.10) as shown in Figures 3-6. \square

Lemma 2.2. (1) When $g < -c^2/(4a_0)$, (1.11) has no equilibria;

(2) When $g = -c^2/(4a_0)$, (1.11) has a unique equilibrium, which is a cusp lying at $P_7(c/(2a_0), 0)$;

(3) When $-c^2/(4a_0) < g$, (1.11) has exactly two equilibria $P_{\pm}((c \pm \sqrt{c^2 + 4a_0g})/(2a_0), 0)$.

In the case that $-c^2/(4a_0) < g < 0$, P_+ is a saddle (resp. center) and P_- is a center (resp. saddle) if $B < 0$ (resp. $B > 0$). In the case that $g > 0$, Both P_+ and P_- are centers (resp. saddles) if $B > 0$ (resp. $B < 0$).

The phase portraits are given in Figure 7.

Proof. In order to analyze system (1.11), which has a singular line $\phi = 0$, we change it into

$$\frac{d\phi}{d\zeta} = B\phi y, \quad \frac{dy}{d\zeta} = -Ay^2 - a_0\phi^2 + c\phi + g, \tag{2.5}$$

by $d\xi = B\phi d\zeta$. Clearly, system (1.11) is equivalent to system (2.5) except on the y -axis.

Consider $g < -c^2/(4a_0)$. From the expression of system (1.11), there is no equilibria. For system (2.5), there exist exactly two equilibria if and only if $A < 0$. Moreover, these two equilibria lie at $\hat{Q}_{\pm}(0, \pm\sqrt{g/A})$. It is not hard to judge that $\hat{Q}_{\pm}(0, \pm\sqrt{g/A})$ are two saddles when $B < 0$ and two nodes when $B > 0$. When $A \geq 0$, system (2.5) has no equilibria.

Consider $g = -c^2/(4a_0)$. Clearly, there exists a unique equilibrium $P_7(c/(2a_0), 0)$ in system (2.5) when $A \geq 0$. When $A < 0$, system (2.5) has three equilibria, which lie at $P_7(c/(2a_0), 0)$ and $\tilde{Q}_{\pm}(0, \pm\sqrt{-c^2/(4a_0A)})$. So, P_7 is the unique equilibrium of system (1.11). Further, P_7 is a degenerate equilibrium and \tilde{Q}_{\pm} are two saddles (resp. nodes) if $B < 0$ (resp. $B > 0$). In order to judge the type of P_7 , by $v = \phi - c/(2a_0)$, $w = (2a_0/c)\phi y$, $t = Bc/(2a_0)\zeta$ we change (2.5) into

$$\frac{dv}{dt} = w, \quad \frac{dw}{dt} = -\frac{2a_0^2}{Bc}v^2 \left(1 + \frac{2a_0}{c}v\right) + w^2 \left(\frac{2a_0}{c} \frac{1}{1 + \frac{2a_0}{c}v} - \frac{2a_0A(c+2a_0)}{Bc^2} \frac{1}{(1 + \frac{2a_0}{c}v)^2}\right). \tag{2.6}$$

By [33, P. 132, Theorem 7.3], O of (2.6) is a cusp, so does P_7 of (1.11). Conclusion (2) is proven.

Similarly to the case $g = -c^2/(4a_0)$, we analyze the cases $-c^2/(4a_0) < g < 0$ and $g > 0$, respectively, and obtain results in conclusion (3). For simplicity, we omit the proof here. \square

Lemma 2.3. For system $(1.12)_{n=2m+1}(m \geq 1)$,

(1) when either $a_0 < 0$ or $a_0 > 0, |g| > \sigma$, there exists a unique equilibrium, which lies at $P_8(\mu_1, 0)$. Moreover, P_8 is a center (resp. saddle) if $a_0B > 0$ (resp. $a_0B < 0$);

(2) when $a_0 > 0$ and $g = \sigma$, there are two equilibria, which lie at $P_9(\mu_2, 0)$ and $P_{10}(\mu_3, 0)$. Moreover, P_9 is a cusp and P_{10} is a center (resp. saddle) if $B > 0$ (resp. $B < 0$);

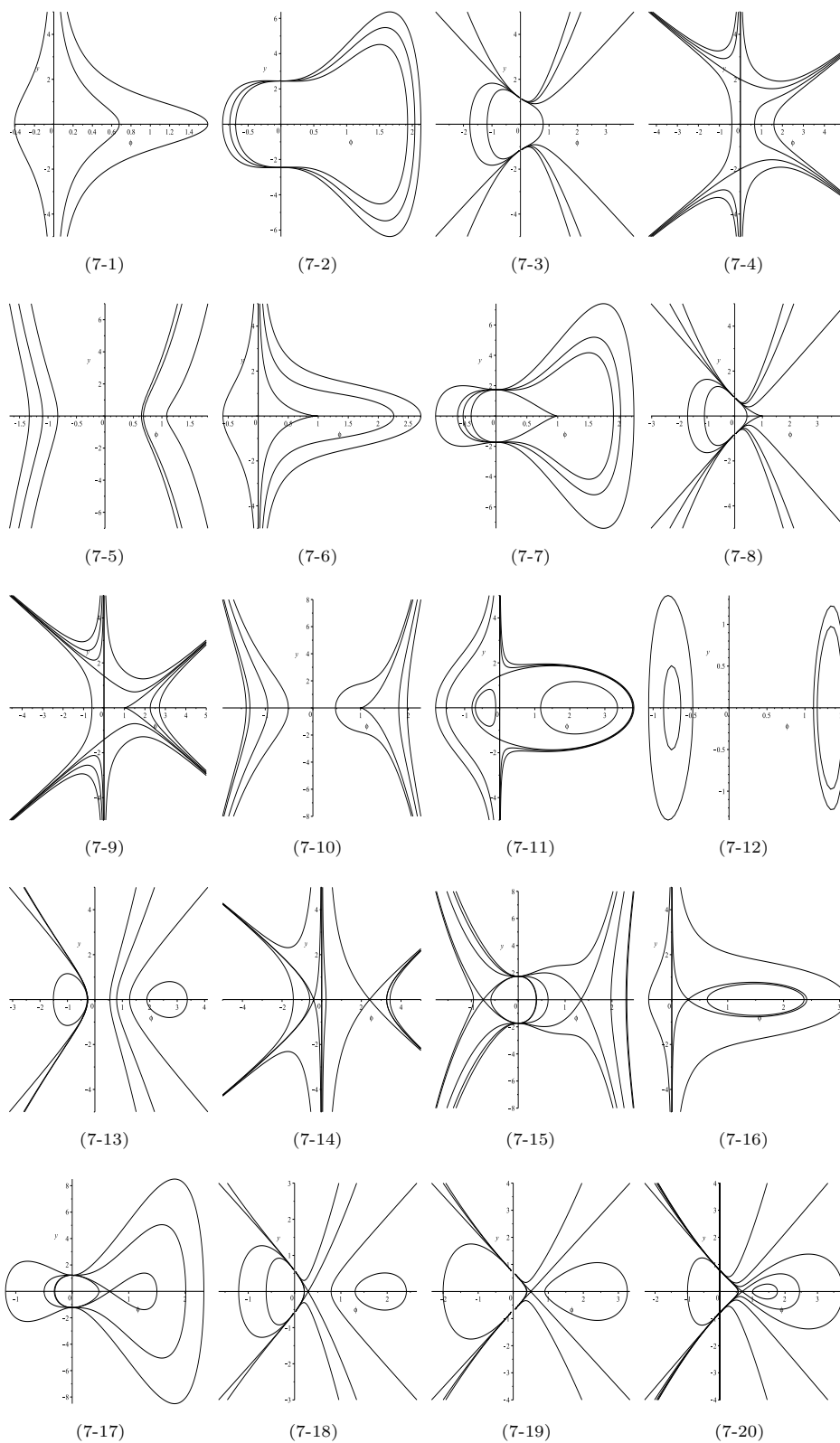


Figure 7. Phase portraits of system (1.11).

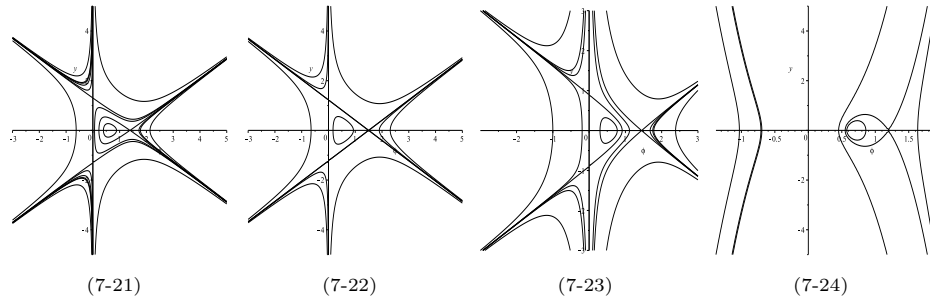


Figure 7. (Continued)

- (3) when $a_0 > 0$ and $g = -\sigma$, there are two equilibria, which lie at $P_{11}(\mu_4, 0)$ and $P_{12}(\mu_5, 0)$. Moreover, P_{12} is a cusp and P_{11} is a center (resp. saddle) if $B > 0$ (resp. $B < 0$);
- (4) when $a_0 > 0$ and $0 < |g| < \sigma$, there are three equilibria, which lie at $P_{13}(\mu_6, 0)$, $P_{14}(\mu_7, 0)$ and $P_{15}(\mu_8, 0)$. Moreover, P_{13} and P_{15} are two centers (resp. saddles) and P_{14} is a saddle (resp. center) if $B > 0$ (resp. $B < 0$),

where $\sigma := 2mc(c/(a_0(2m + 1)))^{1/(2m)}/(2m + 1)$, all $\mu_i (i = 1, \dots, 8)$ are the real zeros of $-a_0\mu^{2m+1} + c\mu + g$ in different cases and satisfy $\mu_2 < \mu_3, \mu_4 < \mu_5, \mu_6 < \mu_7 < \mu_8$. The phase portraits are given in Figure 8.

Proof. We change system (1.12) into

$$\frac{d\phi}{d\zeta} = B\phi^{n-1}y, \quad \frac{dy}{d\zeta} = -A\phi^{n-2}y^2 - a_0\phi^n + c\phi + g \tag{2.7}$$

by $d\xi = B\phi^{n-1}d\zeta$. Clearly, system (1.12) are equivalent to system (2.7) except on the y -axis. We observe that equilibria of system (2.7) _{$n=2m+1$} ($m \geq 1$) lie on ϕ -axis. On the other hand, $(\mu, 0)$ is an equilibrium if and only if μ is a zero of function $f_1(\mu) := -a_0\mu^{2m+1} + c\mu + g$. Notice that $f'_1(\mu) = -a_0(2m + 1)\mu^{2m} + c$, which has no real zeros when $a_0 < 0$ and exactly two real zeros when $a_0 > 0$ at $\mu_1^* := -(c/(a_0(2m + 1)))^{1/(2m)}$ and $\mu_2^* := (c/(a_0(2m + 1)))^{1/(2m)}$. It is easy to check that $f_1(\pm\infty) \rightarrow \mp\infty$ and the function $f_1(\mu)$ is monotonically decreasing in intervals $(-\infty, \mu_1^*)$ and $(\mu_2^*, +\infty)$ while it is monotonically increasing in interval (μ_1^*, μ_2^*) if $a_0 > 0$. Similarly, $f_1(\pm\infty) \rightarrow \pm\infty$ and $f_1(\mu)$ is strictly monotonically increasing on \mathbb{R} if $a_0 < 0$.

Consider that either $a_0 < 0$ or $a_0 > 0, |g| > \sigma$. Since $f_1(\mu)$ has a unique real zero and it is nonzero, denoted by μ_1 , system (2.7) has a unique equilibrium $P_8(\mu_1, 0)$. Straight computation shows that the characteristic equation corresponding to P_8 is $\lambda^2 - B\mu_1^{2m}f'_1(\mu_1) = 0$. Since $f'_1(\mu_1) > 0$ when $a_0 < 0$, P_8 is a center (resp. saddle) if $B < 0$ (resp. $B > 0$). Since $f'_1(\mu_1) < 0$ when $a_0 > 0$ and $|g| > \sigma$, P_8 is a center (resp. saddle) if $B > 0$ (resp. $B < 0$). Conclusion (1) is proven. Similarly to the case $a_0 > 0, g = \sigma$ of Lemma 2.2, we can prove conclusions (2), (3) and (4). So we omit their proofs. \square

Lemma 2.4. For system (1.12) _{$n=2m$} ($m \geq 2$),

- (1) when $g < -\varrho$, there is no equilibria;

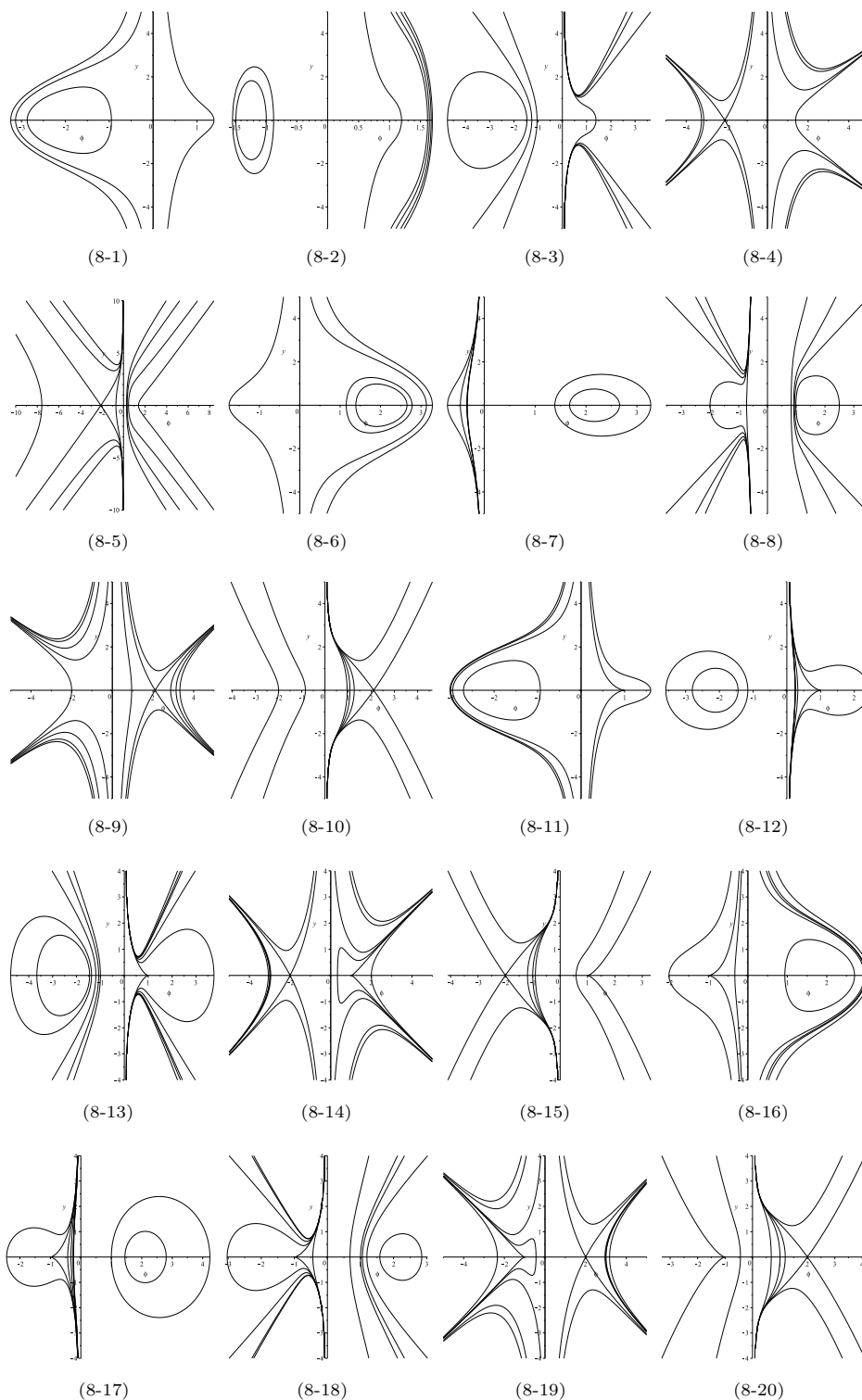


Figure 8. The phase portraits of system (1.12) for $n = 2m + 1 \geq 3$.

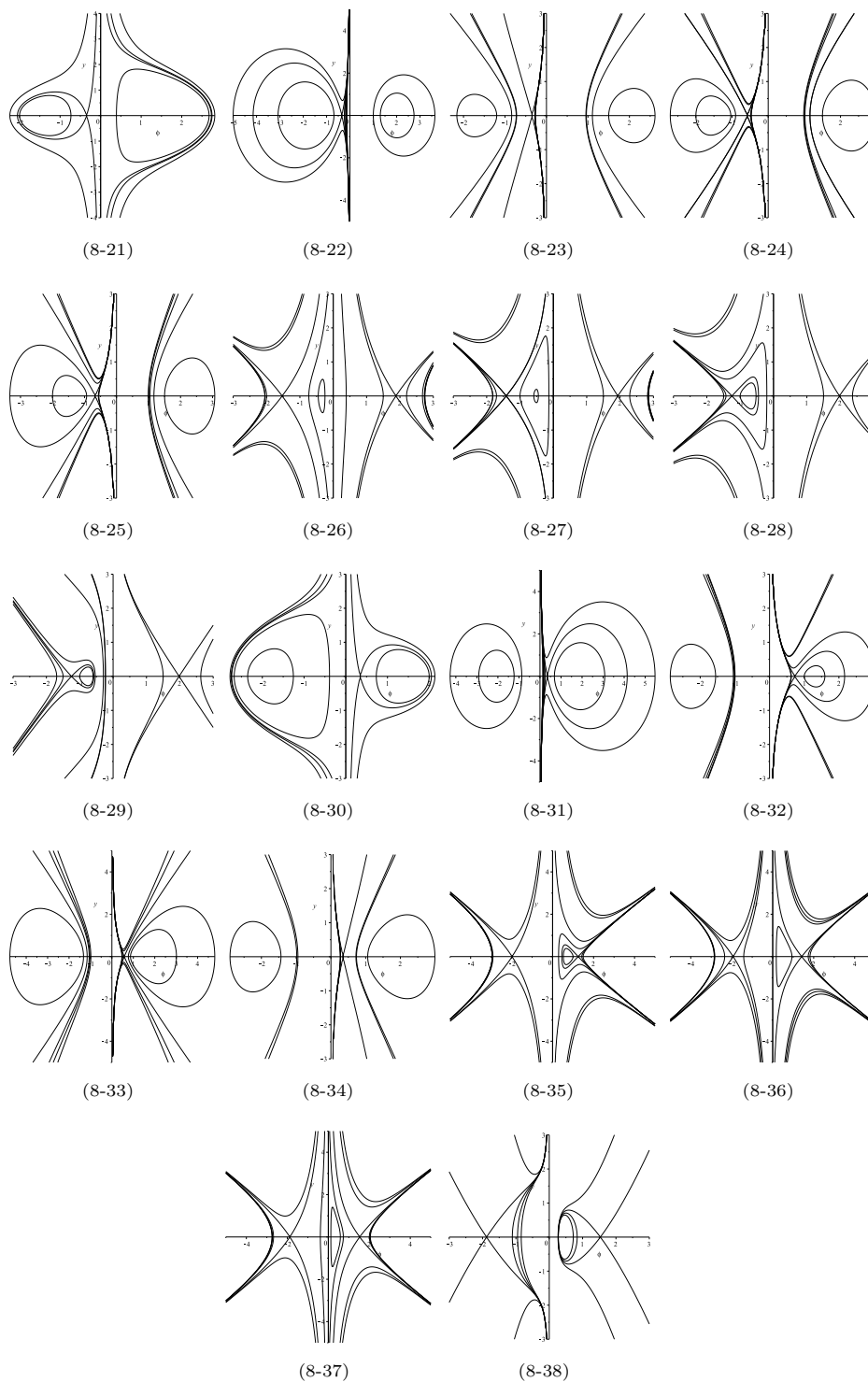


Figure 8. (Continued)

- (2) when $g = -\varrho$, there exists a unique equilibrium, which is a cusp lying at $P_{16}((c/(2ma_0))^{1/(2m-1)}, 0)$;
- (3) when $-\varrho < g < 0$, there exist exactly two equilibria, which lie at $P_{17}(\nu_1, 0)$ and $P_{18}(\nu_2, 0)$. Moreover, P_{17} is a saddle (resp. center) and P_{18} is a center (resp. saddle) if $B > 0$ (resp. $B < 0$);
- (4) when $g > 0$, there exist exactly two equilibria, which lie at $P_{19}(\nu_3, 0)$ and $P_{20}(\nu_4, 0)$. Moreover, P_{19} and P_{20} are two centers (resp. two saddles) if $B > 0$ (resp. $B < 0$),

where $\varrho := (2m - 1)c(c/(2ma_0))^{1/(2m-1)}/(2m)$, all $\nu_i (i = 1, 2, 3, 4)$ are the real zeros of $-a_0\nu^{2m} + c\nu + g$ in different cases and satisfy $\nu_1 < \nu_2, \nu_3 < \nu_4$. The phase portraits are given in Figure 9.

Proof. We observe that equilibria of system (2.7) _{$n=2m$} ($m \geq 2$) lie on the ϕ -axis. On the other hand, $(\nu, 0)$ is an equilibrium if and only if ν is a zero of function $f_2(\nu) := -a_0\nu^{2m} + c\nu + g$. Notice that $f_2'(\nu) = -2ma_0\nu^{2m-1} + c$, which has a unique real zero $\nu^* := (c/(2ma_0))^{1/(2m-1)}$. One can check that $f_2(\pm\infty) \rightarrow -\infty$ and $f_2(\nu)$ is monotonically increasing in $(-\infty, \nu^*)$ while it is monotonically decreasing in $(\nu^*, +\infty)$.

Similarly to the proof of Lemma 2.3, we obtain the number and position of equilibria of system (2.7) _{$n=2m$} by analyzing the zeros of $f_2(\nu)$ in different cases. And then, the types of these equilibria are gotten via their characteristic equations and the monotonicity of f_2 at its zeros, i.e., the results in conclusion (1)-(4). So, we omit the proof. \square

Proof of Theorem 1.1. To prove this theorem, we only need to get wave graphs by all phase portraits given in Figures 3-9. One can obtain the compacton in Figure 1(1-1) from the oval orbit in Figure 3(3-1) which is tangent to the singular straight line $\phi = 0$. The periodic waves in Figures 1(1-2)-(1-4) can be concluded from periodic orbits on both sides of the singular line $\phi = 0$ and the periodic orbit passing through the straight line $\phi = 0$ in Figure 4(4-1), respectively. From the bounded arch orbits between the saddle and the straight line $\phi = 0$ in Figure 7(7-23) and its symmetric picture with respect to this straight line, respectively, periodic cusp waves are obtained in Figures 1(1-5)-(1-6). Analogously, we get the solitary waves in Figures 1(1-7)-(1-10) from the homoclinic orbits in Figures 7(7-16), 7(7-21), 8(8-21) and 8(8-28), respectively. Solitary cusp waves in Figures 1(1-11)-(1-12) are concluded from the straight line orbits between the saddle and the straight line $\phi = 0$ in Figure 7(7-22) and its symmetric picture with respect to $\phi = 0$, respectively. From unbounded arch orbits in Figure 4(4-1), respectively, two-sided breaking waves in Figure 1(1-13)-(1-14) are got. Finally, we obtain the one-sided breaking kink/anti-kink waves in Figures 1(1-15)-(1-18) from the four arch orbits connecting saddles and closing the straight line $\phi = 0$ in Figure 4(4-4), respectively. Thus, each wave graph in Figure 1 corresponds to some certain orbit in these phase portraits given in Figures 3-9. Similarly, for each unbounded wave graph in Figure 2 we can also find a corresponding orbit in these phase portraits given in Figures 3-9. So far, we finish the existence of these wave graphs given in Figures 1 and 2.

On the other hand, we get all wave graphs from orbits in these phase portraits given in Figures 3-9 and find no other wave graphs except those given in Figures 1 and 2. The proof is finished. \square

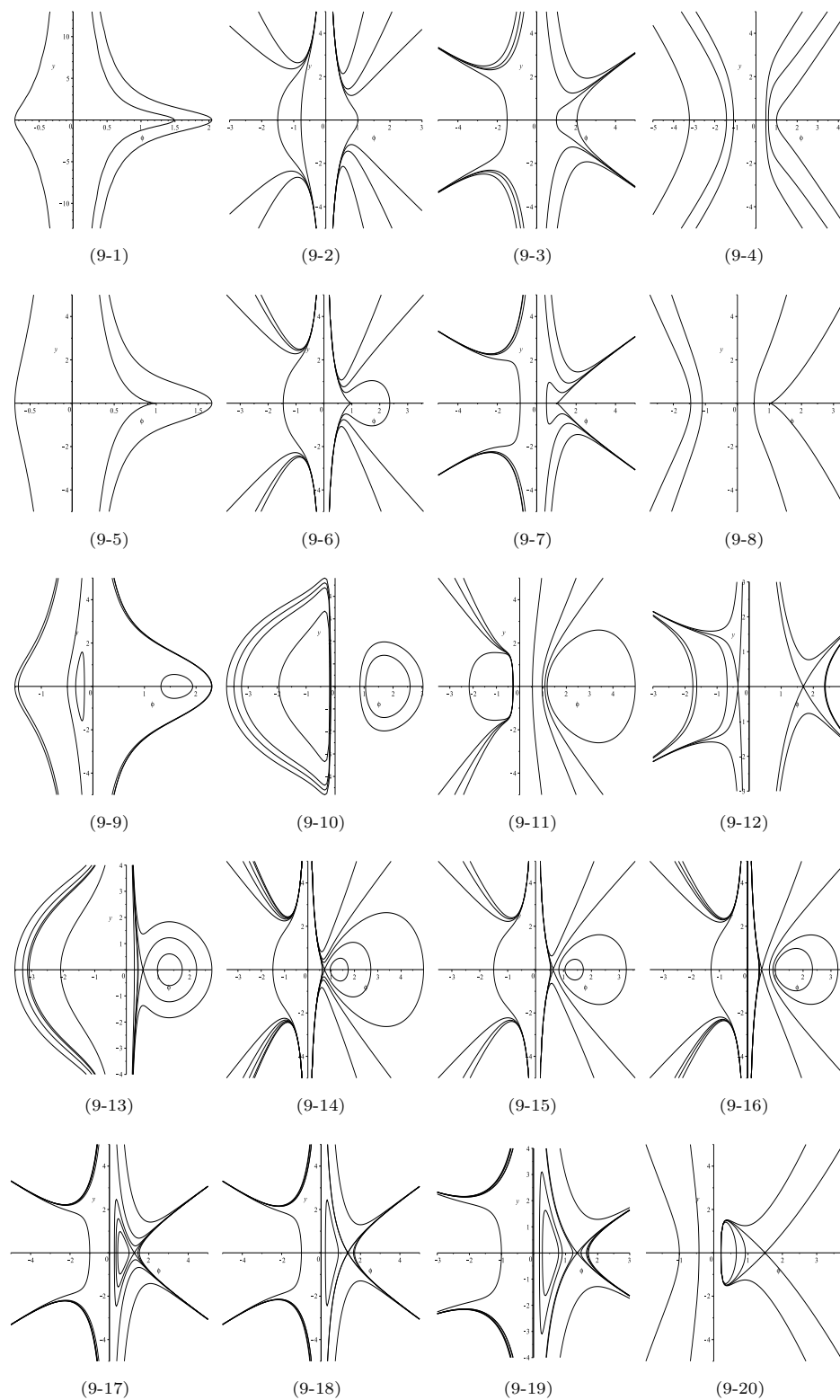


Figure 9. The phase portraits of system (1.12) for $n = 2m \geq 4$.

3. Proof of Theorem 1.2

Using results of phase portrait analysis given in last section, in this section we give expression for bounded traveling wave solutions of equation (1.4). Clearly, system (1.6) has a first integral

$$H(\phi, y) = B\phi^{(2A/B)-(n-2)} \left(\frac{1}{2}\phi^{n-2}y^2 + \frac{a_0}{2(A+B)}\phi^n - \frac{c}{2A-(n-3)B}\phi - \frac{g}{2A-(n-2)B} \right) \quad (3.1)$$

when $A \neq -B, (n-2)B/2, (n-3)B/2$. When $n = 2$, first integral (3.1) is rewritten as

$$H(\phi, y) = B\phi^{2A/B} \left(\frac{1}{2}y^2 + \frac{a_0}{2(A+B)}\phi^2 - \frac{c}{2A+B}\phi - \frac{g}{2A} \right). \quad (3.2)$$

Proof of Theorem 1.2. Taking $A = B/2 > 0$ and $g = 0$, by (3.2) we get that the oval orbit in Figure 3(3-1) which is tangent to the singular straight line $\phi = 0$ is determined by $y^2 = 2a_0(3c/(2a_0) - \phi)\phi/(3B)$. This oval orbit is called a *degenerate homoclinic orbit* as in [13]. Then, it follows from the first equation in (1.8) we obtain expression (1.13) for a compacton solution.

Taking $A = -3B/2 < 0$ and $g = 0$, by (3.2) we get that the family of periodic orbits in Figure 3(3-4) is determined by $y^2 = -2h_1(\phi - r_1)(r_2 - \phi)\phi/B, 0 < r_1 < c/a_0 < r_2, -a_0^2/(2c) < h_1 < 0$. It follows from the first equation in (1.8) we obtain expression (1.14) for a periodic wave solution.

Taking $A = B/2 < 0$ and $-3c^2/(16a_0) < g < 0$, by (3.2) we get that the bounded arch orbit between the saddle and the straight line $\phi = 0$ in Figure 7(7-23) is determined by $y^2 = -2a_0\phi^2/(3B) + c\phi/B + 2g/B$. Then, it follows from the first equation in (1.11) we obtain expression (1.15) for a periodic cusp wave solution.

Taking $A = -3B/2 > 0$ and $-c^2/(4a_0) < g < 0$, by (3.2) we get that the homoclinic orbit in Figure 7(7-24) is determined by $y^2 = 2h_2(\phi - r_3)(r_4 - \phi)^2/B, 0 < r_3 < (c - \sqrt{c^2 + 4a_0g})/(2a_0) < r_4 = (c + \sqrt{c^2 + 4a_0g})/(2a_0), h_2 = -(4a_0^3g + 3a_0^3cr_4)/(3c^3 + 9a_0cg + 3(c^2 + a_0g)^{3/2})$. It follows from the first equation in (1.11) we obtain (1.16) for a solitary traveling wave solution.

Taking $A = B/2 < 0$ and $g = -3c^2/(16a_0)$, by (3.2) we get that these straight line orbits between the saddle and the straight line $\phi = 0$ in Figure 7(7-22) is determined by $y = \pm\sqrt{2a_0/(-3B)}(\phi - 3c/(4a_0))$. Then, it follows from the first equation in (1.11) we obtain expression (1.17) for a solitary cusp wave solutions of valley type (valleyon solutions).

Taking $A = B/2 > 0$ and $g = -c^2/(4a_0)$, by (3.2) we get that the unbounded arch orbits in Figure 7(7-6) which lie in the region sandwiched by the singular line $\phi = 0$ and two stable and unstable manifolds of the cusp P_7 is determined by

$$y^2 = \frac{2a_0(r_5 - \phi) \left(\phi^2 + \left(r_5 - \frac{3c}{2a_0} \right) \phi + \left(r_5^2 - \frac{3c}{2a_0}r_5 + \frac{3c^2}{4a_0^2} \right) \right)}{3B\phi},$$

$0 < r_5 < c/(2a_0)$. Then, it follows from the first equation in (1.11) we obtain the expression (1.18) for a bounded two-sided breaking wave solution. In addition, we also get that the arch orbit connecting the cusp P_7 and closing the singular straight line $\phi = 0$ in one direction on the above of ϕ -axis is determined by $y^2 = 2a_0(c/(2a_0) - \phi)^3/(3B\phi)$ and $y > 0$. Then, we obtain expression (1.19) for a one-sided breaking kink wave solution. \square

4. Conclusions and simulations

Using the approach of dynamical systems, in this paper we study traveling solutions for the ZK($n, 2n, -n$) equation (1.4) with 6 parameters a_0, b_0, c_0, a, c, g . In Theorem 1.1, for (1.4) with $a^2 \neq b_0/c_0$ and $ac \neq 0$ we get 7 classes of bounded traveling waves including compacton, periodic wave, periodic cusp wave, solitary wave, solitary cusp wave, two-sided breaking wave and one-sided breaking kink/anti-kink wave. Moreover, there is no other bounded traveling waves. In Theorem 1.2, we give 7 expressions for these seven classes of bounded traveling wave solutions.

We observe that the phase portraits in Figures 3-9 have different topological structures, which means that bifurcations happen for planar differential systems when parameters vary. Accordingly, these traveling waves appear, disappear or evolve into each other when parameters vary.

Remark 4.1. For $n = 2, B = 1, g = 0$, referring to Figures 3(3-1)-(3-4), we find that equation (1.4) with $a^2 \neq b_0/c_0$ and $ac \neq 0$ has a compacton and a family of periodic waves when $A > -1/2$ but there is only a family of periodic waves when $A \leq -1/2$. That is, a compacton appears when A changes from $-1/2$ into a greater number.

For $n = 4, B = 1, g = 0$, referring to Figures 5(5-1)-(5-2), we find that equation (1.4) with $a^2 \neq b_0/c_0$ and $ac \neq 0$ has a family of periodic waves and a family of two-sided breaking waves when $A = 1/2$. The family of two-sided breaking waves still exists but some periodic waves become another family of two-sided breaking waves when A changes from $1/2$ into a greater number.

For $n = 2, A = B = -1, -c^2/(4a_0) < g < 0$, referring to Figures 7(7-21)-(7-23), we find that equation (1.4) with $a^2 \neq b_0/c_0$ and $ac \neq 0$ has a solitary cusp wave when $g = -2c^2/(9a_0)$, and this solitary cusp wave becomes a solitary wave (resp. a periodic cusp wave) when g changes from $-2c^2/(9a_0)$ into a less number (resp. greater number). Moreover, there appear a family of two-sided breaking waves, a one-sided breaking kink wave and a one-sided breaking anti-kink wave when g changes from $-2c^2/(9a_0)$ into a greater number.

By fixing parameters in different parameter bifurcation sets and taking proper initial values, we simulate 18 types of bounded traveling waves and 10 types of unbounded traveling waves of system (1.5) in Figures 1 and 2, respectively.

Fixing $n = 2, A = 1/2, B = a_0 = c = 1, g = 0$, we get the simulation of compacton as shown in Figure 1(1-1) if we take the initial values $\phi(0) = 1.5$ and $\phi'(0) = 0$, the simulation of periodic wave as shown in Figure 1(1-2) if we take the initial values $\phi(0) = 0.6$ and $\phi'(0) = 0$, and the simulations of two-sided breaking waves as shown in Figures 1(1-13)-(1-14) if we take the initial values $\phi(0) = 2, \phi'(0) = 0$ and $\phi(0) = -0.8, \phi'(0) = 0$, respectively.

Fixing $n = 3, A = B = a_0 = 1, c = 3, g = 0$, we get the simulation of periodic wave as shown in Figure 1(1-3) if we take the initial values $\phi(0) = -2$ and $\phi'(0) = 0$, and the simulations of periodic cusp waves as shown in Figures 1(1-5)-(1-6) if we take the initial values $\phi(0) = \pm 2.449489742$ and $\phi'(0) = 0$.

Fixing $n = 3, A = 1/2, B = a_0 = -1, c = 3, g = 0$, we get the simulation of periodic wave as shown in Figures 1(1-4) taking the initial values $\phi(0) = 1$ and $\phi'(0) = 0$.

Fixing $n = 2, A = -1/2, B = a_0 = -1, c = 2, g = 1/2$, we get the simulation of solitary wave as shown in Figure 1(1-7) taking the initial values $\phi(0) = -1 -$

$\sqrt{2}, \phi'(0) = 0$.

Fixing $n = 2, A = -3/2, B = 1, a_0 = -1, c = 4, g = 3$, we get the simulation of solitary wave as shown in Figure 1(1-8) taking the initial values $\phi(0) = -3/4, \phi'(0) = 0$.

Fixing $n = 2, A = 1/2, B = a_0 = 1, c = 2, g = -1/2$, we get the simulation of solitary wave as shown in Figure 1(1-9) taking the initial values $\phi(0) = 1 + \sqrt{2}, \phi'(0) = 0$.

Fixing $n = 2, A = 3/2, B = -1, a_0 = 1, c = 4, g = -3$, we get the simulation of solitary wave as shown in Figure 1(1-10) taking the initial values $\phi(0) = 3/4, \phi'(0) = 0$.

Fixing $n = 2, A = -1/2, B = -1, a_0 = 1, c = 2, g = -3/4$, we get the simulation of solitary cusp wave as shown in Figure 1(1-11) taking the initial values $\phi(0) = 0.00001, \phi'(0) = 0$.

Fixing $n = 2, A = 1/2, B = 1, a_0 = -1, c = 2, g = 3/4$, we get the simulation of solitary cusp wave as shown in Figure 1(1-12) taking the initial values $\phi(0) = -0.00001, \phi'(0) = 0$.

Fixing $n = 3, A = B = -1, c = 3, g = 0$, we get the simulations of one-sided breaking kink waves as shown in Figures 1(1-15)-(1-16) if we take the initial values $\phi(0) = 1, \phi'(0) = \sqrt{2}$ and $\phi(0) = -1, \phi'(0) = -\sqrt{2}$, and the simulations of one-sided breaking anti-kink waves as shown in Figures 1(1-17)-(1-18) if we take the initial values $\phi(0) = 1, \phi'(0) = -\sqrt{2}$ and $\phi(0) = -1, \phi'(0) = \sqrt{2}$.

References

- [1] A. Biswas, *1-soliton solution of the generalized zakharov-kuznetsov equation with nonlinear dispersion and time-dependent coefficients*, Physics Letters A, 2009, 373(33), 2931–2934.
- [2] A. Biswas and E. Zerrad, *Solitary wave solution of the zakharov-kuznetsov equation in plasmas with power law nonlinearity*, Nonlinear Anal.: Real World Appl., 2010, 11(4), 3272–3274.
- [3] C. Deng, *New exact solutions to the zakharov-kuznetsov equation and its generalized form*, Comm. Nonlinear Sci. Num. Simul., 2010, 15(4), 857–868.
- [4] Z. Du, Z. Feng and X. Zhang, *Traveling wave phenomena of n-dimensional diffusive predator-prey systems*, Nonlinear Anal.: Real World Appl., 2018, 41, 288–312.
- [5] Y. Fu and J. Li, *Bifurcations of travelling wave solutions in three modified Camassa-Holm equations*, J. Appl. Anal. Comput., 2021, 11(2), 1051–1061.
- [6] A. Johnpillai, A. Kara and A. Biswas, *Symmetry solutions and reductions of a class of generalized (2+1)-dimensional zakharov-kuznetsov equation*, Int. J. Nonlinear Sci. Num. Simul., 2011, 12(1–8), 45–50.
- [7] T. Kano and T. Nishida, *A mathematical justification for korteweg-de vries equation and boussinesq equation of water surface waves*, Osaka J. Math., 1986, 23(2), 389–413.
- [8] D. Korteweg and G. de Vries, *On the change of form of long waves advancing in a rectangular canal, and on a new type of long stationary waves*, Philosophical Magazine, 1895, 39(240), 422–443.

- [9] S. Lai, J. Yin and Y. Wu, *Different physical structures of solutions for two related zakharov-kuznetsov equations*, Physics Letters A, 2008, 372(43), 6461–6468.
- [10] J. Li, *Geometric properties and exact travelling wave solutions for the generalized Burger-Fisher equation and the Sharma-Tasso-Olver equation*, J. Nonlinear Model. Anal., 2019, 1(1), 1–10.
- [11] J. Li and G. Chen, *On a class of singular nonlinear traveling wave equations*, Int. J. Bifurcation and Chaos, 2007, 17(11), 4049–4065.
- [12] B. Li, Y. Chen and H. Zhang, *Exact traveling wave solutions for a generalized zakharov-kuznetsov equation*, Appl. Math. Comput., 2003, 146(2–3), 653–666.
- [13] J. Li, J. Wu and H. Zhu, *Traveling waves for an integrable higher order kdv type wave equations*, Int. J. Bifurcation and Chaos, 2006, 16(08), 2235–2260.
- [14] J. Li, Y. Zhang and J. Liang, *Bifurcations and exact traveling wave solutions for a new integrable nonlocal equation*, J. Appl. Anal. Comput., 2021, 11(3), 1588–1599.
- [15] A. Ludu and J. Draayer, *Patterns on liquid surfaces: cnoidal waves, compactons and scaling*, Physica D: Nonlinear Phen., 1998, 123(1–4), 82–91.
- [16] P. Meuris and F. Verheest, *Korteweg-de vries equation for magnetosonic modes in dusty plasmas*, Physics Letters A, 1996, 219(5–6), 299–302.
- [17] S. Munro and E. Parkes, *The derivation of a modified zakharov-kuznetsov equation and the stability of its solutions*, J. Plasma Physics, 1999, 62(3), 305–317.
- [18] P. Rosenau, *Nonlinear dispersion and compact structures*, Phys. Rev. Lett., 1994, 73(13), 1737–1741.
- [19] P. Rosenau and J. Hyman, *Compactons: solitons with finite wavelength*, Phys. Rev. Lett., 1993, 70(5), 564–567.
- [20] F. Tappert and C. Varma, *Asymptotic theory of self-trapping of heat pulses in solids*, Phys. Rev. Lett., 1970, 25(16), 1108–1111.
- [21] A. Wazwaz, *Compactons and solitary patterns structures for variants of the KdV and the KP equations*, Appl. Math. Comput., 2003, 139(1), 37–54.
- [22] A. Wazwaz, *An analytic study of Compactons structures in a class of nonlinear dispersive equations*, Math. Comput. Simul., 2003, 63(1), 35–44.
- [23] A. Wazwaz, *Special types of the nonlinear dispersive zakharov-kuznetsov equation with compactons, solitons, and periodic solutions*, Int. J. Comp. Math., 2004, 81(9), 1107–1119.
- [24] A. Wazwaz, *Exact solutions with solitons and periodic structures for the zakharov-kuznetsov (zk) equation and its modified form*, Comm. Nonlinear Sci. Num. Simul., 2005, 10(6), 597–606.
- [25] A. Wazwaz, *Explicit traveling wave solutions of variants of the $k(n,n)$ and the $zk(n,n)$ equations with compact and noncompact structures*, Appl. Math. Comput., 2006, 173(1), 213–230.
- [26] A. Wazwaz, *The extended tanh method for the zakharov-kuznetsov (zk) equation, the modified zk equation, and its generalized forms*, Comm. Nonlinear Sci. Num. Simul., 2008, 13(6), 1039–1047.

-
- [27] M. Wei and S. Yang, *Periodic traveling wave solutions of $zk(2,4,-2)$ equation*, J. Advances in Math. Comp. Sci., 2014, 4(13), 1849–1856.
- [28] S. Wu and G. Chen, *Uniqueness and exponential stability of traveling wave fronts for a multi-type SIS nonlocal epidemic model*, Nonlinear Anal.: Real World Appl., 2017, 36, 267–277.
- [29] B. Xia, Z. Qiao and J. Li, *An integrable system with peakon, complex peakon, weak kink, and kink-peakon interactional solutions*, Comm. Nonlinear Sci. Num. Simul., 2018, 63, 292–306.
- [30] E. Yomba, *Jacobi elliptic function solutions of the generalized zakharov-kuznetsov equation with nonlinear dispersion and t -dependent coefficients*, Physics Letters A, 2010, 374(15–16), 1611–1615.
- [31] N. Zabusky and M. Kruskal, *Interaction of solitons in a collisionless plasma and the recurrence of initial states*, Phys. Rev. Lett., 1965, 15(6), 240–243.
- [32] V. Zakharov and E. Kuznetsov, *On threedimensional solitons*, Zhurnal Eksp. Teoret. Fiz., 1974, 66, 594–597.
- [33] Z. Zhang, T. Ding, W. Huang and Z. Dong, *Qualitative Theory of Differential Equations*, Transl. Math. Monogr., Amer. Math. Soc., Providence, RI, 1992.